AD-A186 162   RADAR ECHO SIGNATURES VERSUS RELATIVE PRECIPITATION(U)   1/1
AIR FORCE INST OF TECH WRIGHT-PATTERSON AFB OH
T A HUBER 1987 AFIT/CI/NR-87-114T

UNCLASSIFIED   F/G 17/9   NL

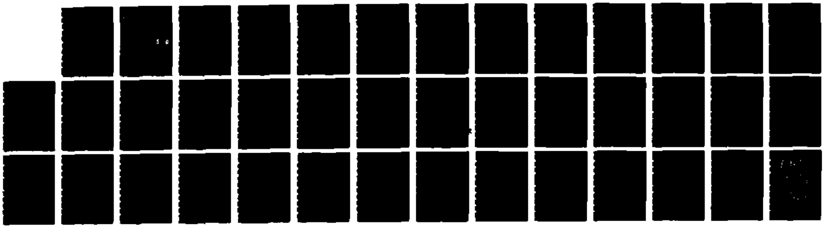

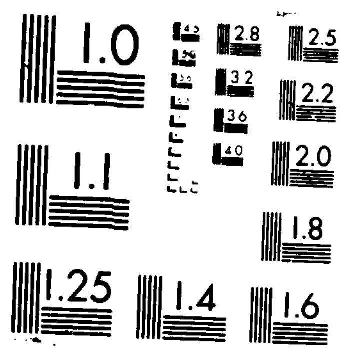

ROCOPY RESOLUTION TEST CHART

AD-A186 162 DTIC FILE COPY

UNCLASSIFIED

SECURITY CLASSIFICATION OF THIS PAGE (When Data Entered)

REPORT DOCUMENTATION PAGE

READ INSTRUCTIONS BEFORE COMPLETING FORM

1. REPORT NUMBER: AFIT/CI/NR 87-114T	2. GOVT ACCESSION NO.
3. RECIPIENT'S CATALOG NUMBER	
4. TITLE (and Subtitle): Radar Echo Signatures Versus Relative Precipitation	5. TYPE OF REPORT & PERIOD COVERED: THESIS/DISSERTATION
6. PERFORMING ORG. REPORT NUMBER	
7. AUTHOR(s): Terry Alvin Huber	8. CONTRACT OR GRANT NUMBER(s)
9. PERFORMING ORGANIZATION NAME AND ADDRESS: AFIT STUDENT AT: Texas A&M University	10. PROGRAM ELEMENT, PROJECT, TASK AREA & WORK UNIT NUMBERS
11. CONTROLLING OFFICE NAME AND ADDRESS: AFIT/NR WPAFB OH 45433-6583	12. REPORT DATE: 1987
	13. NUMBER OF PAGES: 2[illegible]
14. MONITORING AGENCY NAME & ADDRESS (if different from Controlling Office)	15. SECURITY CLASS. (of this report): UNCLASSIFIED
	15a. DECLASSIFICATION/DOWNGRADING SCHEDULE

16. DISTRIBUTION STATEMENT (of this Report)

APPROVED FOR PUBLIC RELEASE; DISTRIBUTION UNLIMITED

DTIC ELECTE NOV 1 8 1987 S D

17. DISTRIBUTION STATEMENT (of the abstract entered in Block 20, if different from Report)

18. SUPPLEMENTARY NOTES

APPROVED FOR PUBLIC RELEASE: IAW AFR 190-1

Lynn Wolaver 2 Sep 87

LYNN E. WOLAVER
Dean for Research and Professional Development
AFIT/NR

19. KEY WORDS (Continue on reverse side if necessary and identify by block number)

20. ABSTRACT (Continue on reverse side if necessary and identify by block number)

ATTACHED

DD FORM 1 JAN 73 1473 EDITION OF 1 NOV 65 IS OBSOLETE

SECURITY CLASSIFICATION OF THIS PAGE (When Data Entered)

87 10 28 175

RADAR ECHO SIGNATURES VERSUS RELATIVE PRECIPITATION

A Thesis

by

TERRY ALVIN HUBER

Submitted to the Graduate College of
Texas A&M University
in partial fulfillment of the requirements for the degree of

MASTER OF SCIENCE

December 1987

Major Subject: Meteorology

RADAR ECHO SIGNATURES VERSUS RELATIVE PRECIPITATION

A Thesis

by

TERRY ALVIN HUBER

Approved as to style and content by:

James R. Scoggins
(Chairman of Committee)

George L. Huebner
(Member)

Jeffrey D. Hart
(Member)

James R. Scoggins
(Head of Department)

December 1987

ABSTRACT

Radar Echo Signatures Versus Relative Precipitation (December 1987)
Terry Alvin Huber, B.S., Angelo State University
Chairman of Advisory Committee: Dr. James R. Scoggins

The objective of this study is to show the relationship between cell-echo signatures and precipitation characteristics, and to support the hypothesis that, during the lifespan of any particular isolated convective cell, the relative rainfall rate, as determined by radar for a given volume scan and averaged over horizontal area of the radar echo, is related to characteristics of echo-profiles of average reflectivity (dBz) and horizontal area, as defined by the 10-dBz contour.

The data used were collected during the Texas HIPLEX (High Plains Cooperative Program) field experiment of 1979. Four isolated cases, two rainshowers and two thundershowers, were selected for study.

Profiles from volume scans taken 10 minutes before, during, and 10 minutes after the maximum radar-determined rainfall rate, averaged over horizontal area of the echo for each case, were examined for signatures relative to the time of occurrence of this maximum average. The following tentative conclusions were reached based on the small sample.

a. Average reflectivity and radar-derived average rainfall rate

Three conclusions can be drawn concerning the average reflectivity profile of an isolated convective cell and the radar-determined average rainfall rate of the same cell:

1) If the radar reflectivity from the cell, averaged for each level within a volume scan, produces an echo profile which exhibits the highest values at mid levels, then the maximum average rainfall rate determined by radar has not yet occurred.

2) If, on the other hand, an echo profile reveals only decreasing values of average reflectivity from the lowest levels to the top of the echo, then either the maximum average rainfall rate determined by radar is occurring or has occurred.

3) No identifiable characteristic (i.e., change in slope), can distinguish an average reflectivity profile produced during the time of maximum average radar-determined rainfall rate from one produced after this time, except a decrease in magnitude at all levels.

b. Horizontal area and radar-derived average rainfall rate

Two conclusions can be drawn concerning the horizontal area profile of an isolated convective cell and the radar-determined average rainfall rate of the same cell.

1) If an echo from the cell produces a profile of horizontal area, as defined by the 10-dBz closed contour, that indicates greater horizontal area at mid levels, then the maximum average rainfall rate as determined by radar has not yet occurred.

2) No identifiable characteristic distinguishes the horizontal area profile during the time of maximum average radar-determined rainfall rate from one after this time.

DEDICATION

This thesis is dedicated to my father and mother, Alvin B. Huber and Mary L. Huber. Although taken from us in death while in the prime of his life, Dad's memory is indelible and daily occupies a special place in the author's thoughts. Dad's meticulous nature, together with his rare analytical ability to tackle even the most difficult of tasks, often left his young son, the author, silently watching and learning in awe. Mom's dedication towards perfection and her constant encouragement during many discouraging times served as a catalyst to kindle a now burning desire for achievement. Her Christian values and deeds instilled in the author an unfaltering love for God and mankind.

Without this positive influence and their guidance, college, let alone this advanced degree, would not have been a reality. To them both the author will remain grateful for all eternity.

ACKNOWLEDGEMENTS

The author wishes to acknowledge the following individuals for their support: Dr. James R. Scoggins for his encouragement, direction, and patience during all phases of this thesis; Dr. George L. Huebner for his help in locating the data tapes and reviewing this thesis; Dr. Jeffrey D. Hart for his guidance and willingness to serve as a committee member, and; Jackie Strong for all her secretarial help and for the typing of the final draft of this thesis.

The author wishes to acknowledge the United States Air Force for providing the opportunity and financial support for this advanced degree through the Civilian Institution Programs branch of the Air Force Institute of Technology.

The author wishes to give special acknowledgement to his wife Barbara for her caring support, devotion, and love during his pursuit of this Master of Science Degree.

TABLE OF CONTENTS

LIST OF FIGURES

1. INTRODUCTION

From the very beginning of meteorology, man has been faced with the nagging question: Will it rain? Meteorologists predict the onset and amount of precipitation from large and well-developed systems. However, pinpointing the same for an isolated convective cell is extremely challenging. Rainshowers or thundershowers may appear rather suddenly and move over any particular area. Some of these cells release no measurable precipitation as they pass over an area while others do. Consequently, meteorologists must have some means of distinguishing one from the other.

To answer the question of whether a particular cloud will produce measurable precipitation at any given location, a tool is needed to monitor the evolutionary processes of and within the cell. Radar is well suited for this purpose. Once hydrometeors within the cloud attain minimum detectable size, the cloud's evolution may be tracked using radar. The lifecycle of cell echoes, from initial detection to dissipation, has been well documented. As the liquid water content of the cloud continues to increase, so too, proportionally, does radar reflectivity (Battan, 1973). Assuming that the temperature profile of the environment favors continued cell growth, rising parcels will continue to supply the cloud with liquid water. Thus, the radar signature will be seen to enlarge horizontally and vertically. From this point the cloud's dimensions may continue to increase; again, if environmental conditions are favorable. Now, if at some time in the cell's life, the amount of liquid water present exerts a gravitational force which is greater than the positive buoyancy force, the liquid water in the cloud will begin to fall through the cloud base as rain. Correspondingly, a noticeable decrease in the cell's echo signature will be observed, especially in the cloud's upper half. In order for the precipitation to

---

The Journal of the Atmospheric Sciences was used as a model for this thesis.

actually reach the ground, the sub-cloud layer must be sufficiently saturated or thin.

As clouds form, they may undergo many different stages of development. Although cells may eventually merge and form multi-cell units, this study concentrated only on single cells which remained isolated from other cells during their life.

The study of cloud precipitation processes is extremely important. With each new study of this type, the knowledge base is broadened. New techniques must be found to aid the operational meteorologist in his decisions concerning precipitation. With that purpose in mind, this study was undertaken.

2. OBJECTIVE

The objective of this study is to show the relationship between cell-echo signatures and precipitation characteristics, and to support the hypothesis that, during the lifespan of any particular isolated convective cell, the relative rainfall rate, as determined by radar for a given volume scan and averaged over horizontal area of the radar echo, is related to characteristics of echo-profiles of average reflectivity (dBz) and horizontal area, as defined by the 10-dBz contour.

3. BACKGROUND

An adequate understanding of the time variation of hydrometeors within isolated convective cells must be obtained before any attempt is made to apply radar data to cloud physics research. During the development stage, which can range from 10 to 20 minutes, the condensation-coalescence process dominates for those cumuli which form in temperatures above 0 degrees C (Dennis and Kosciepski, 1972; Battan, 1973). All cases identified in this study had initial echoes which formed above this temperature. Any increase in reflectivity observed during this initial stage was, therefore, attributed to an increase in the detectable liquid water within the cloud and not to spurious returns produced by ice or hail.

In studying the processes involved in cloud physics, the researcher has several tools from which to select. Of these, the two most common are data collection and computer modeling. Data collection consists primarily of either on-site or remote sampling. On-site sampling is usually accomplished by instrument laden aircraft sampling different parameters while penetrating selected clouds. However, this technique is not used routinely and has limited availability. On the other hand, radar serves to supply data which can be displayed quickly for analysis and which is readily available to most forecasters in the field. For this reason it was chosen as a means by which the objective of this research might be fulfilled.

Over the past few years, several indepth studies have been conducted to investigate the dependence of radar-determined rainfall upon radar echo characteristics of individual cells. Of these, one is most applicable to this study. In their paper, Gagin, Rosenfeld, and Lopez (1985) investigated several of these relationships. Using data collected during FACE (Florida Area Cumulus Experiment), 349 convective cells were identified and tracked over their lifetimes. Only single cells were considered in their research. Applying regression analyses to the data, they examined the relationships between maximum vertical dimensions and other cell properties, such as maximum cell horizontal area, maximum cell reflectivity, and various precipitation parameters. Based on their

findings, they concluded that "cell rainfall and area are strongly related," and "the evolution of precipitation in a convective cell is such that its radar echo dimensions are interrelated not only to size but also in their rates of formation." Additionally, they found the rainfall rate to be dependent upon the observed echo strength.

When using radar data, the temporal and spatial variation of the drop size distribution of the hydrometeors within the sampled cloud must be considered. Warner (1977) noted, using aircraft to sample selected clouds, that the drop size distribution within isolated cumuli remained essentially constant over time and space. Also, he observed that the profile of liquid water content, for a given horizontal slice through a cloud, displayed a "top-hat" rather than a Gaussian profile. Both of these findings are very important to any work involving the use of radar data to study the variability of liquid water content over space and time. As is well documented by Battan (1973), the energy reflected back to the radar receiver from any cell is highly dependent upon the drop size distribution and the amount of detectable liquid water within the cell.

Another study done by Lopez et al. (1984) showed a relationship between several echo characteristics. They examined the relationship between cell horizontal area and duration as well as cell reflectivity and duration. They saw a positive correlation between each of these. Thus, considering this and assuming convective cells of longer duration would precipitate more, as did Malkus and Simpson (1964), the relationship between precipitation and a cloud's physical dimensions becomes evident.

The majority of precipitation producing clouds are small isolated cells (Lopez, 1978). These small isolated cells have horizontal areas of 50 km^2 or less. Thus, on a daily basis, operational meteorologists at the local level are more often confronted with the variation of precipitation from these small isolated convective cells rather than from larger composite systems.

4. DATA AND ANALYSIS

a. Radar characteristics and data retrieval

Conventional radar data were used in this research. The data were collected during the Texas HIPLEX (High Plains Cooperative Program) field experiment of 1979. The general HIPLEX area was defined by the region bounded by San Angelo, Midland, Lubbock, and Abilene. The radar used for the data collection was the Skywater radar provided by the U.S. Bureau of Reclamation. The Skywater radar was located in Big Spring and scanned the entire HIPLEX region.

The Skywater radar was developed by the Bureau to be used for cloud modification and cloud physics research. It is a 5.4 cm wavelength unit with a beam width of 1-degree (Riggio et al., 1983). It is very well suited for collecting data to be used in cloud studies. For each degree of azimuth a total of 250 bins were recorded. Each bin was 0.5 km deep. Thus, the radar had an effective range of 125 km. The first 20 bins or 10 km were not used due to ground clutter.

The radar was operated in several scan modes. The monitor (MON) mode was used if none of the HIPLEX research aircraft was flying. The other three modes were used when the aircraft were flying a HIPLEX mission. Normally, the scan modes recorded complete volume scans from 1 degree to 12 degrees (Riggio et al., 1983). This mode, it was found, produced an elapsed time of 10 minutes between the start of each new volume scan. Occasionally, a mode was selected which recorded volume scans from 1 degree to 20 degrees during a time interval of 5 minutes. One of the cases chosen for this study was recorded under this latter scan mode. A digital-video-integrator-processor (DVIP) unit was incorporated in the radar to process the data before storing it on magnetic tape. The raw data were then processed and compressed into A-file format tapes.

b. Computer processing of A-file data tapes

A-file tapes for selected days were ordered from the Bureau of Reclamation and computer programs were developed for processing the data on a 24-bit Harris main-frame computer operated by the meteorology department at Texas A&M University. As the tapes were written in 32-bit format, special techniques were used to read or "buffer" the data into a buffer file which could then be operated on by standard FORTRAN (Formula Translation) code.

Each tape contained two major pieces of information. For every whole degree of azimuth from 1 to 360 degrees, hereafter referred to as radial, header information was given along with the corresponding DVIP values for that particular header. Each header contained the year, Julian day, recording time [given in Greenwich Mean Time (GMT)], radial degree, antenna elevation angle, and the number of subfields or DVIP groups for that header. All bins along each radial with DVIP values less than 32, a value considered to be the threshold level, were not recorded from the original raw data tapes onto the compressed A-file tapes. Consequently, each header was followed by DVIP information of variable length. Because of this variability, the subfield information contained within each header proved invaluable for developing the computer programs used.

The FORTRAN algorithm used for processing the data from computer tape to final printed output contained several steps. At every step, care was taken to validate the resulting numbers by hand. The general sequence proceeded as follows.

a) For each radial the DVIP values were placed in a one-dimensional array containing 250 elements. Thus, each element was equivalent to a bin having approximate horizontal dimensions of ½ km by ½ km.

b) Each of the DVIP values in the array were converted to Z-values of reflectivity using the following standard radar equations which contain some values unique to the skywater radar (Huebner, 1987):

1) $dBm = A + BX + CX^2 + DX^3$
   where the coefficients A, B, C, and D have the values -112.097, $.24766$, $.68282 \times 10^{-3}$, and -0.15317×10^{-5}, respectively.
2) $dBz = dBm + 20 \log(r/r_0) + 88.3$
   where r is the range in km, r_0 is the 10 km range blanking, and 88.3 is the radar constant.
3) $Z_e = 10^{(dBz/10)}$
   where Z_e is the effective radar reflectivity factor and is defined by the relationship $Z_e = \Sigma n_i D_i^6$.

c) Each radial containing the new Z-values was then adjusted for antenna elevation by projecting it onto the horizontal using a cosine function. This step, which was included to reduce the error in estimating the distance through a cloud along a radial when the beam path is not parallel to the earth's surface, required occasional averaging between two adjacent bins depending on the elevation angle.

d) After projection onto the horizontal, every other Z-value along the radial was averaged with its adjacent neighbor, therefore reducing the number of bins to 125.

e) For a given elevation angle and chosen quadrant, Z-values for successive radials were assigned into a two-dimensional array using an r,Θ to x,y transformation routine. This routine averaged Z-values between radials as needed to produce a two-dimensional representation of a horizontal slice through the atmosphere. Each number contained in every element within this new array represented an averaged Z-value for a horizontal area of 1 km^2.

f) Finally, each Z-value in the array was converted back to a dBz value, and the array was then printed on paper for further detailed hand analysis.

c. Case identification and tracking

Identified cases had to meet certain criteria. As mentioned earlier, only single convective cells which remained totally isolated from other cells during their lifetimes were chosen. Because the radar beam experiences attenuation as it passes through liquid water, only those cells which had no detectable liquid water between them and the radar site were chosen. Also, only cases exhibiting detectable liquid water in the lowest elevations, indicating precipitation falling through the cloud base, were chosen. No cells were chosen which were more than 50 km from the radar site. This last criterion was imposed to reduce errors in rainfall rate estimates due to range bias as described by Battan (1973).

Once these criteria were established, cells were identified as potential cases and tested for acceptability under the criteria. Several days were identified which had produced the most convective activity within the HIPLEX area for 1979. The potential cases were then selected from these more active days. A computer printout of the lowest level for the first volume scan was generated for each potential case, and the criteria applied. This process continued for each volume scan. If a volume scan exhibited any feature which was unacceptable under the criteria, then the cell was rejected as a case. The chosen cases were then tracked through their lifespans.

Tracking of each case was accomplished by using printouts of all levels for each volume scan recorded during the life of the cell. Tracking was initiated when the first dBz value above the threshold of 10 dBz was observed at any level and continued until no values above this limit were observed on the lowest level.

d. Analysis

Each level printed for a given day, time, and elevation angle was not unlike that which would have been displayed by the Skywater's PPI (Planned Position Indicator) scope. As a further check, these printed representations of the PPI display were compared to actual 16 mm film

reels of the Skywater's PPI scope. As expected the printed levels matched the PPI film display very well. Thus, confidence was gained that the computer generated printouts for each level truly represented the reflectivity field as recorded and displayed on the Skywater radar's PPI scope.

Once each case was chosen, a detailed analysis of each volume scan, recorded throughout the life of that particular cell, could be conducted. To accomplish this, a series of printouts for each level were printed which employed a finer grid size for more detail. Each level was printed employing a computer-generated square grid with each dBz value located at the center of each grid box. The grid was scaled so that ½ in represented 1 km. For each printed level, an isoline representing the 10-dBz contour was drawn. The 10-dBz threshold value was chosen to represent the minimum reflectivity level. Thus, any dBz value below 10 was not only rejected as background noise, but not printed. Based on Warner's observation of the "top-hat" profile of liquid water within small cumuli, it was assumed that this 10-dBz contour represented the outer fringes of the cloud (1977). Therefore, the horizontal area enclosed by this contour represented the horizontal area in km^2 of the cloud for any given level. This convention of using the 10-dBz contour was consistent with the procedures used by Gagin, Rosenfeld, and Lopez (1985) on the FACE data. Depending on the scan mode, as described earlier, each volume scan produced either 12 or 20 printed levels for hand contouring and further analysis.

Further calculations were performed to produce single representative values of average reflectivity and horizontal area for each of the levels within a volume scan, along with estimates of the average rainfall rate for each volume scan. The dBz values within the grid boxes enclosed by the 10-dBz contour on each level were again converted to Z-values of effective radar reflectivity factor (z_e). These z_e values were then integrated over a horizontal area to obtain a single average effective Z-value ($\overline{Z_e}$) for each level. The integration was performed using the expression

$$\overline{Z_e} = \int \frac{z_e \, dA}{N} \cong \frac{\overset{N}{\Sigma} z_e}{N}$$

where $\overline{Z_e}$ is the average effective radar reflectivity factor for that level, N is the total horizontal area, dA is a unit area in the horizontal plane, and z_e is each effective Z-value bounded within the 10-dBz contour. The single $\overline{Z_e}$ value for each level was then converted back to a dBz value to be used in plotting profiles later on. Estimates of the height for each level were made by first calculating the distance from the radar to the center of the cell and then applying an above ground level (AGL) estimate routine as described by Battan (1973). Since the cell's position in space changed with time, the cell's distance was recomputed at the start of each new volume scan, as were the AGL estimates. A value for the horizontal area of the cell for each level was obtained by using the scaled grid.

The $\overline{Z_e}$ values obtained for each of the lowest elevation scans were used to compute the instantaneous rainfall rates in mm hr^{-1} for all volume scans recorded during the life of the cell. The HIPLEX Z-R relationship

$$\overline{Z_e} = 200 \, \overline{R^{1.6}}$$

was used to obtain these average rainfall-rate estimates. As the title of this study indicates, the precipitation estimates are relative to a given volume scan. These rainfall rates should, therefore, be considered only in this context. In addition, since these rainfall rates were calculated using Z-values integrated over a horizontal area, they represent average rainfall rates over area. By no means should these estimates be thought of as averages between volume scans or the absolute maximum or minimum over the life of the cell. However, research has shown that, even for sampling intervals having a δt of 10 minutes, the error in rainfall-rate estimates is less than 10 percent (Huebner, 1987). Any further reference to rainfall rates or precipitation, then, represents an average rainfall rate over a horizontal area.

Before any further analysis could be accomplished, it was necessary to construct a graph of these rainfall rates together with height profiles of average reflectivity and horizontal area. An overlay or composite graph, displaying the radar-determined rainfall rates relative to each of the volume scans for every case, was constructed. Rawinsonde data recorded at Big Spring for times closest to the first volume scan for each of the cases were then plotted. From these plotted data, the cloud-base height for each of the chosen cases was estimated by locating the Lifting Condensation Level (LCL). In particular, the approximate height above Mean Sea Level (MSL) in m of the cloud's base could be determined by locating the LCL and then assuming this height defined the height of the cloud base. Then the AGL height was computed by subtracting the MSL height for Big Spring; the MSL height for Big Spring is 873 m. This AGL height for the cloud's base was used, in conjunction with the height values obtained earlier for each level within the cloud, to construct height profiles of average dBz and horizontal area from one volume scan to another.

5. CASE STUDIES

Four cases were identified for this study. Of these, one occurred on 4 June 1979, while the other three were all recorded on 16 July 1979. The 4 June case encompassed a total of 5 volume scans each of 5 minutes in duration with elevation angles from 1 to 20 degrees. The first volume scan began at 2255 GMT, with the last ending at 2320 GMT. The maximum average reflectivity for this cell was 41.06 dBz, and the maximum horizontal area was 50 km^2. The maximum detectable height of the echo was approximately 7,500 m. This cell is typical of the late-afternoon or early-evening thundershower which is quite common in this region of the Texas High Plains. This case will be referred to as Case 1.

The last three cases appeared on the same day and are referred to as Case 2, Case 3, and Case 4, respectively. Each of these three cases produced six 10-minute volume scans recorded through a maximum elevation angle of 12 degrees. Their respective start and stop times were 0016-0116 GMT, 0056-0156 GMT, and 0116-0216 GMT. The maximum values for average dBz and horizontal area, for any level, along with the maximum detected height of the echo were:

	Avg. dBz	Hor. Area (km^2)	Height (m)
Case 2	34.92	21	3839
Case 3	38.12	30	5447
Case 4	35.60	20	7774

Like Case 1, Case 4 represented a thundershower, while Cases 2 and 3 were rainshowers. These four cases produced reflectivity values and horizontal dimensions comparable in magnitude to cells examined by other researchers (Lopez, 1978; Gagin 1980; Gagin, Rosenfeld, and Lopez, 1985).

Figure 1 compares the rainfall-rate curves for all cases. This figure was constructed so that all maximum detected rainfall rates were plotted coincident on the vertical axis. The vertical axis defines the rainfall rate relative to a given volume scan. The horizontal axis

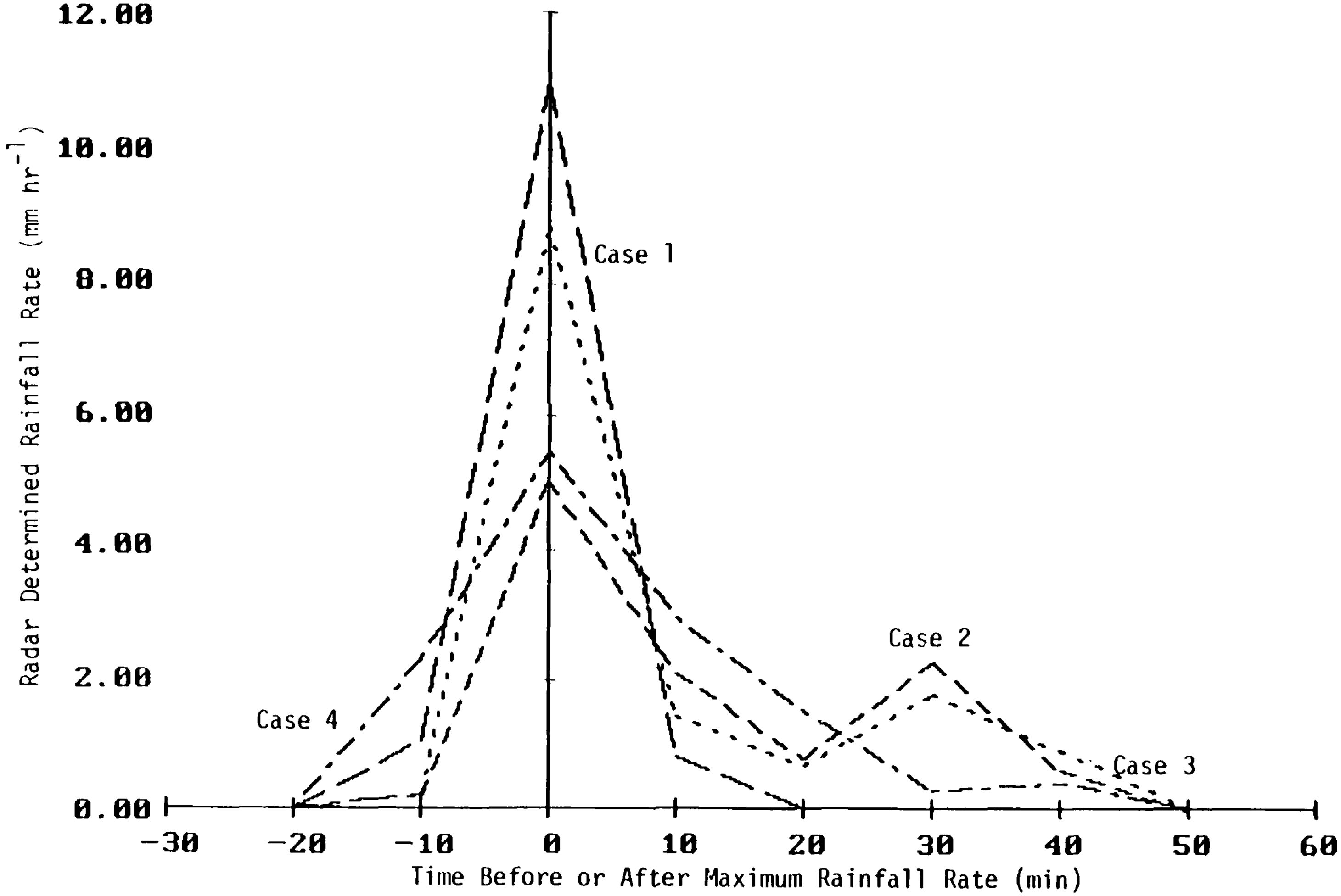

Fig. 1. Time relative to rainfall maximum as a function of radar-determined rainfall rates for successive volume scans. Volume Scans 1, 2, 3, 4, 5, and 6 correspond to Times -10, 0, 10, 20, 30, and 40, respectively.

shows the time before, during, and after the maximum recorded rainfall rates. These times are indicated by a negative sign, zero, or a positive sign, respectively. Since Case 1 had volume-scan intervals different from the other cases, only rainfall rates for Volume Scans 1, 3, and 5 are shown for it. In addition, a fictitious (although reasonable) rainfall rate of 0.00 mm hr^{-1} was included for an interval just before and after the first and last volume scans of each of the cases. This allowed all of the curves in Figure 1 to begin and end on the horizontal axis.

The curves in Figure 1 show similarities. The radar detected and recorded a peak in the rainfall rate on the second volume scan of each of the four cases. This indicates that the majority of the precipitation produced by these cases came within the first 10 to 20 minutes of their lifespans. Two of the cases show maxima slightly above 4.00 mm hr^{-1}, while the other two indicate peak rainfall rates above 8.00 mm hr^{-1}. All further analysis will be presented with respect to these peaks.

The high variability of precipitation observed over the time interval centered around the recorded rainfall maxima was a direct consequence of the dynamic and microphysical processes occurring within the cells. The rather small-scale changes occurring within the cells produced not only different rainfall rates over time, but large-scale changes in their horizontal dimensions at all levels. These dimensional changes in turn appeared as changes in the echoes or signatures of the cells detected by the radar. Changes in echo signatures should, therefore, indicate changes in the radar-determined precipitation rates.

In order to further investigate the relationship between cell echo signatures and precipitation, profiles of average reflectivity and horizontal area for each of the cases were grouped. Profiles were grouped according to their time of occurrence with respect to the precipitation maxima in Figure 1. For example, all four average reflectivity profiles for the volume scans just before the maximum radar-determined rainfall rate appear on one graph, the next four profiles of this same parameter, representing volume scans recorded during the maxima, appear on the next graph, and then the same for the after-maxima

volume scans. These three volume scans of interest are thus indicated by the Times -10, 0 and 10, respectively, on the horizontal axis in Figure 1.

Figure 2 shows the average reflectivity factor profiles for the volume scan just before the rainfall maxima. The vertical axis shows height (AGL) in m, and the horizontal axis shows values of average reflectivity factor in dBz. The solid line above and parallel to the horizontal axis in Figure 2 represents an average height (AGL) for the cloud bases, and was determined to be approximately 1,500 m. For reference, any part of a curve above this line will be considered as part of the cell, and any part below will represent the rainshaft.

In Figure 2 several common features among the profiles of average reflectivity are evident. Every profile displays a maximum or "bulge" close to mid level of the echo. This "bulge" indicates a concentration of detectable liquid water in the cloud. From this mid-level bulge, each case displays a negative slope to the top of the echo. As would be expected, the detectable liquid water content is less at higher levels. Below cloud base, the average reflectivity decreases as altitude decreases. The smaller values shown in the lowest elevation scans indicate small precipitation rates. This is further supported by examining the rainfall rates given for Time -10 (Volume Scan 1) in Figure 1. In each of the cases, the "bulge" in the profiles preceded the maximum precipitation rate. No other common characteristic was distinguishable as a possible flag to indicate the profiles had occurred before the maximum precipitation rate. During the time interval between Volume Scans 1 and 2 (Times -10 and 0 in Figure 1), the distribution of liquid water within the cases changed notably.

The profiles corresponding to Time Zero (Volume Scan 2) in Figure 1 are presented in Figure 3. A downward shift in the average reflectivity maxima, to a position at or close to cloud base, can be seen in all cases. This settling of the average reflectivity "bulge" is a direct consequence of the highest levels, or core, of detectable liquid water moving from a point somewhere near mid cloud to a position closer to cloud base. Also, a significant increase in the average reflectivity

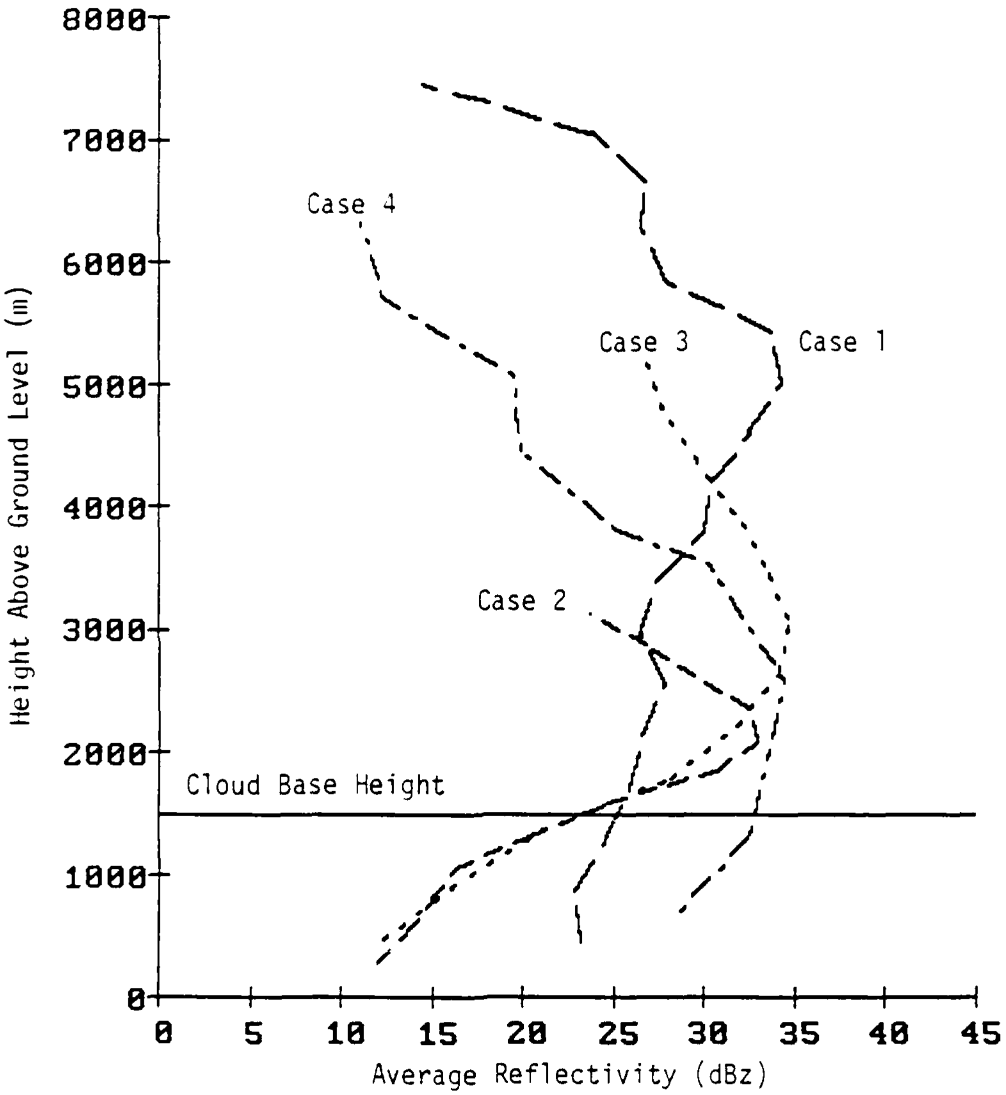

Fig. 2. Profiles of average reflectivity as a function of height recorded one volume scan before the maximum rainfall rate in Fig. 1.

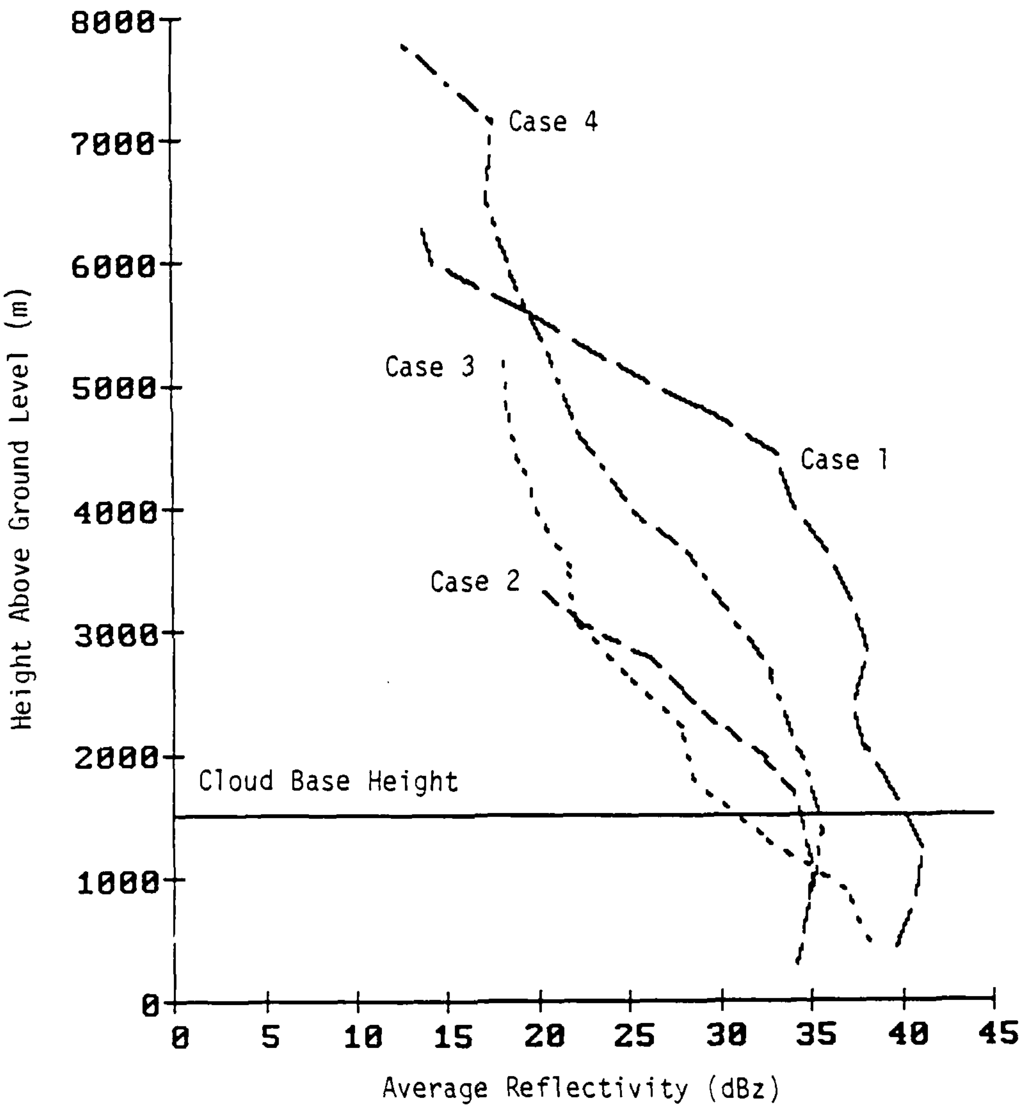

Fig. 3. As in Fig. 2 but for the volume scan recorded during the maximum rainfall rate in Fig. 1.

has occurred at all levels below cloud base for all four cases, indicating a substantial increase in precipitation relative to the previous volume scan.

By the third volume scan (Time 10 in Figure 1), the rainfall rates had diminished. All four cases show sizable decreases in average reflectivity values for all levels (Figure 4). The negative slope in the average reflectivity profiles, which characterizes all four cases at this stage, indicates a massive decrease in liquid water content within the cells. In this latter regard, the small positively-sloped portion at the bottom of the profile for Case 1 presents the only anomaly. This could be a result of the extreme decrease or collapse of liquid water in the upper levels of Case 1 within a short time period. In 10 minutes, Case 1 went from the strongest of any of the cases, in terms of average dBz values for all levels, to the weakest. This sudden collapse could have induced an inward entrainment of drier air into the cell, causing dilution of the saturated air, which drastically reduced the average reflectivity in all but the lowest portions of the cell's rainshaft. Since all the profiles in Figures 3 and 4 have negative slopes except for those levels near the ground, no distinction could be made as to their time of occurrence with respect to rainfall rate. However, they all occurred either during or after the maximum precipitation rate.

As a cell's liquid water content changes, its horizontal dimensions are expected to change as well. This suggests that during cell development the strength of the radar echo and the horizontal area would increase simultaneously. Every cell detected by radar goes through a cycle which can be subdivided into: 1) development stage, where the horizontal area displayed on the PPI scope increases; 2) mature stage, where the horizontal area may change very little, and; 3) dissipation stage, where the horizontal area decreases. Height profiles of horizontal area observed for different volume scans will reflect these changes.

Profiles of horizontal area of the radar echoes are shown in Figure 5. Like Figure 2, the profiles in Figure 5 correspond to Time -10 (Volume Scan 1) in Figure 1. Each profile shows a maximum or bulge close to mid level of the echo. This altitude is a favored location within the cell for increases in average reflectivity and horizontal

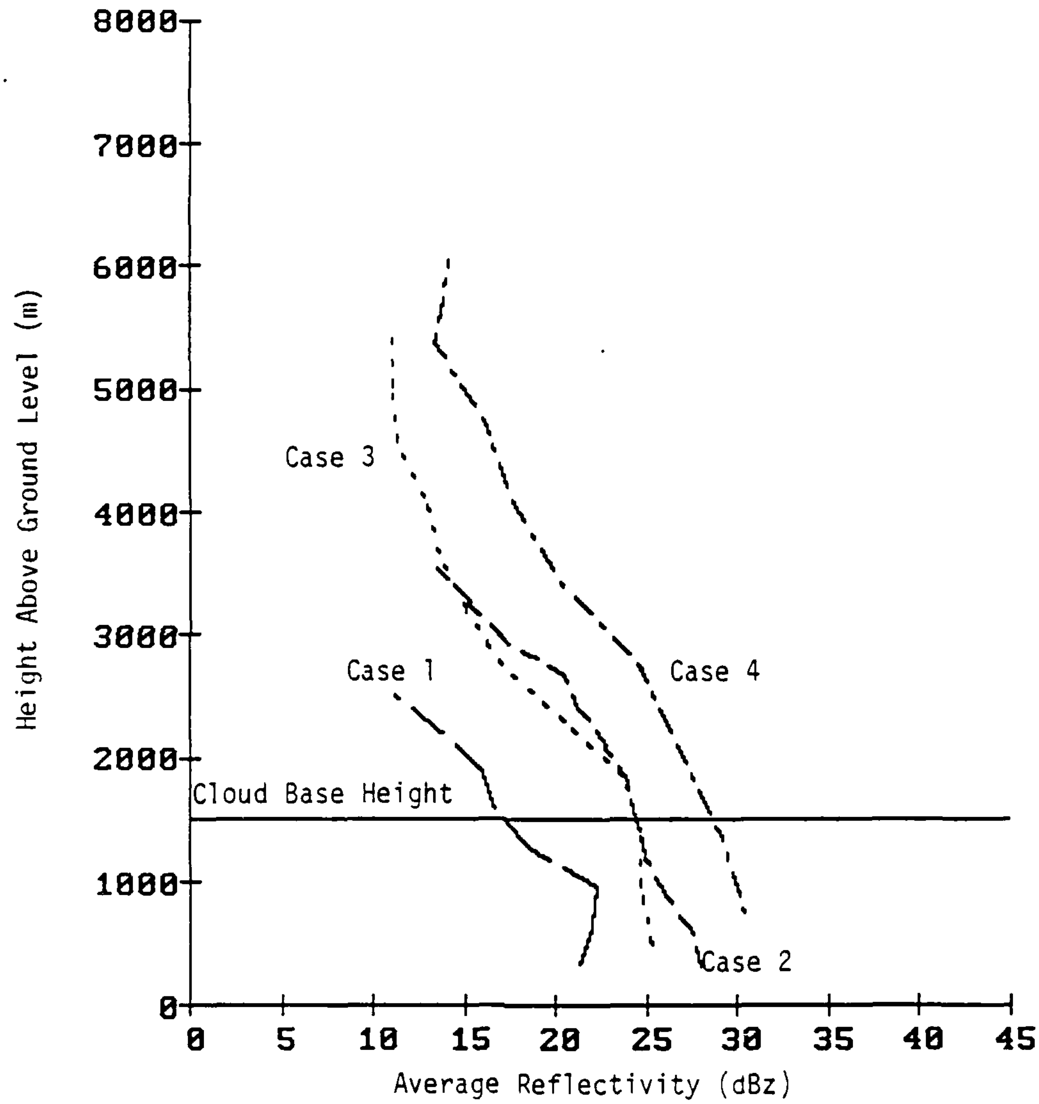

Fig. 4. As in Fig. 2 but recorded one volume scan after the maximum rainfall rate in Fig. 1.

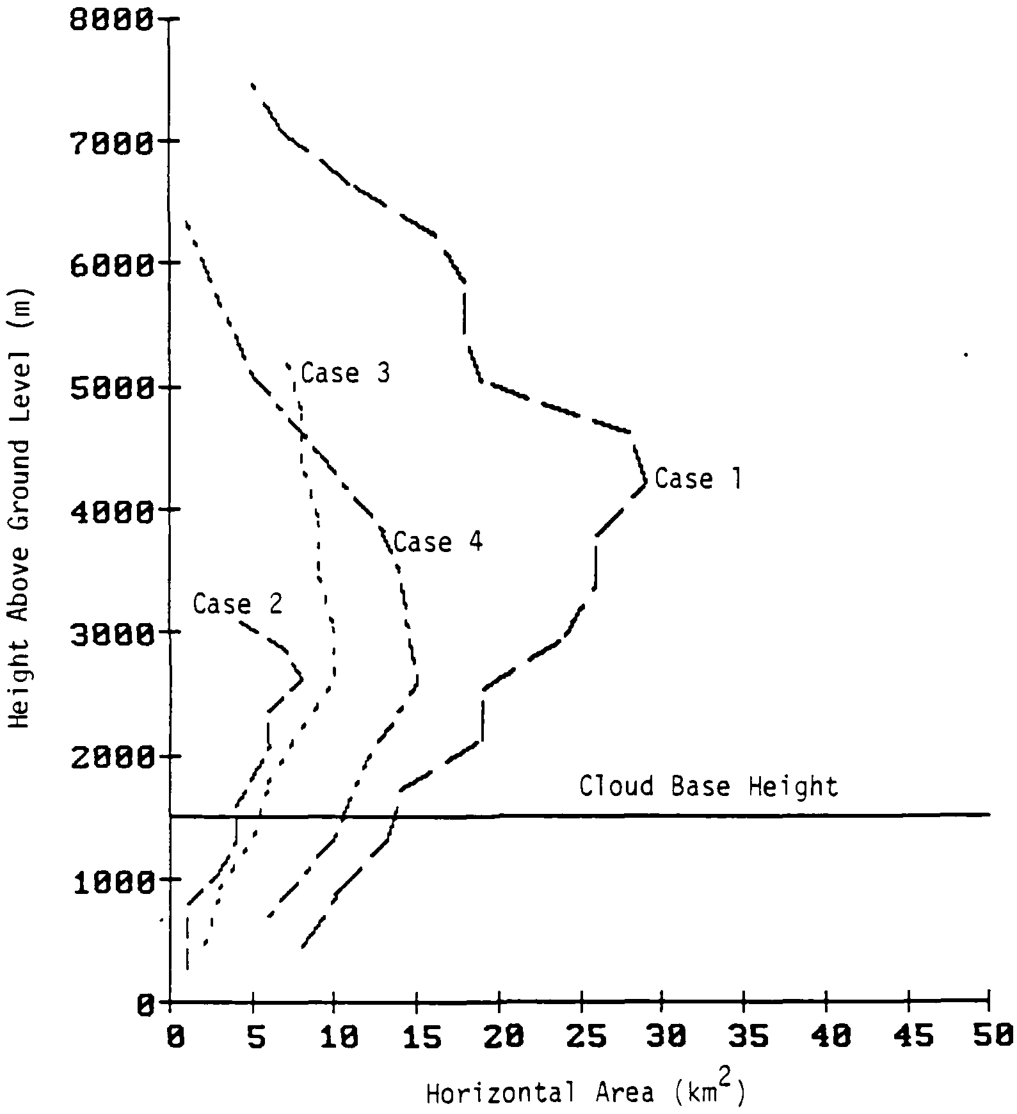

Fig. 5. Profiles of horizontal area as a function of height recorded one volume scan before the maximum rainfall rate in Fig. 1.

area during the development stage. All four cases in Figure 5 presented a bulge or maximum of horizontal area at mid level of the echo as did the average reflectivity factor profiles in Figure 2. Each of these bulges preceded the maximum radar-determined rainfall rate shown for Time Zero in Figure 1.

By the time of maximum radar-determined precipitation (Time Zero in Figure 1), the horizontal area has changed at all scan levels for every case (Figure 6). Although the profiles show no obvious similarities or pattern, they reveal an increase in horizontal area at and just above cloud base for all cases. This increase is especially evident for Case 1. Its horizontal area at cloud base increased from 13 km^2 to 43 km^2 in the 10-minute time interval between Figures 5 and 6 (Volume Scans 1 and 2).

By Volume Scan 3 (Time 10 in Figure 1), the horizontal area at cloud base had continued to change for all the cases (Figure 7). There is a distinct increase in all cases except one. Consistent with the changes occurring between Figures 3 and 4 (Volume Scans 2 and 3), Case 1 again exhibits a total collapse of its horizontal area for all levels. The previous explanation proposed to justify the collapse of the average reflectivity profile appears to apply here as well.

A comment on the maximum radar-determined rainfall rates in Figure 1 is noteworthy here. Two of the Cases, 1 and 3, had distinctly higher rates than the others. Case 1 was a thundershower, and its higher rate is not surprising. However, Case 3 attained only rainshower height as determined by radar. Therefore, its maximum rainfall rate of approximately 8.50 mm hr^{-1} was unexpected.

In an attempt to resolve this, attention should be focused on the changes in horizontal area for Case 3 from Figure 5 to Figure 6. Although the horizontal area at cloud base for Cases 2 and 4 increases only slightly, Case 3 shows a considerable increase. Since the precipitation rates were obtained by integrating z_e over a horizontal area for a given level, an increase in horizontal area, as is seen here, could account for this higher rainfall rate.

The opposite holds true for Case 4. It was identified as a thundershower, but its maximum radar-determined rainfall rate was only

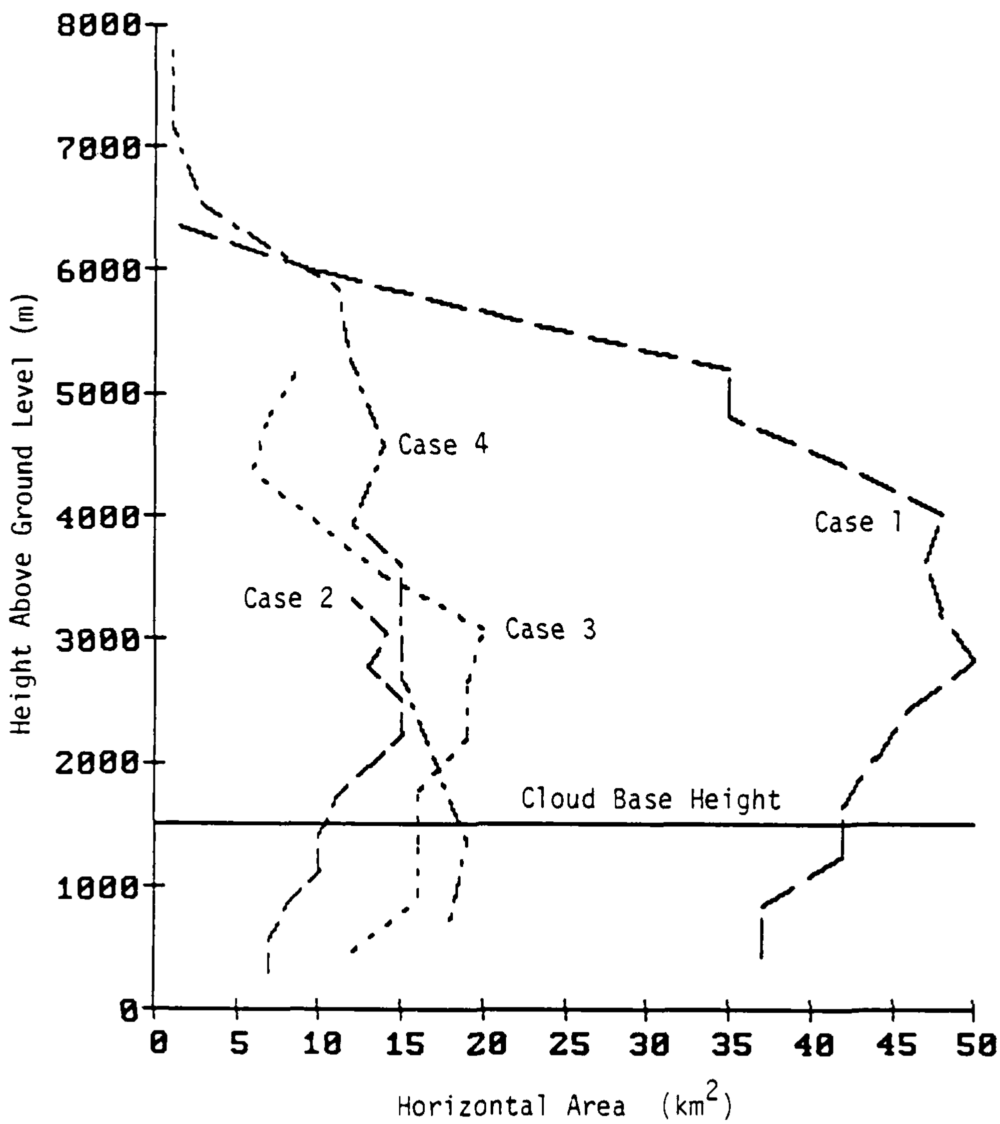

Fig. 6. As in Fig. 5 but for the volume scan recorded during the maximum rainfall rate in Fig. 1.

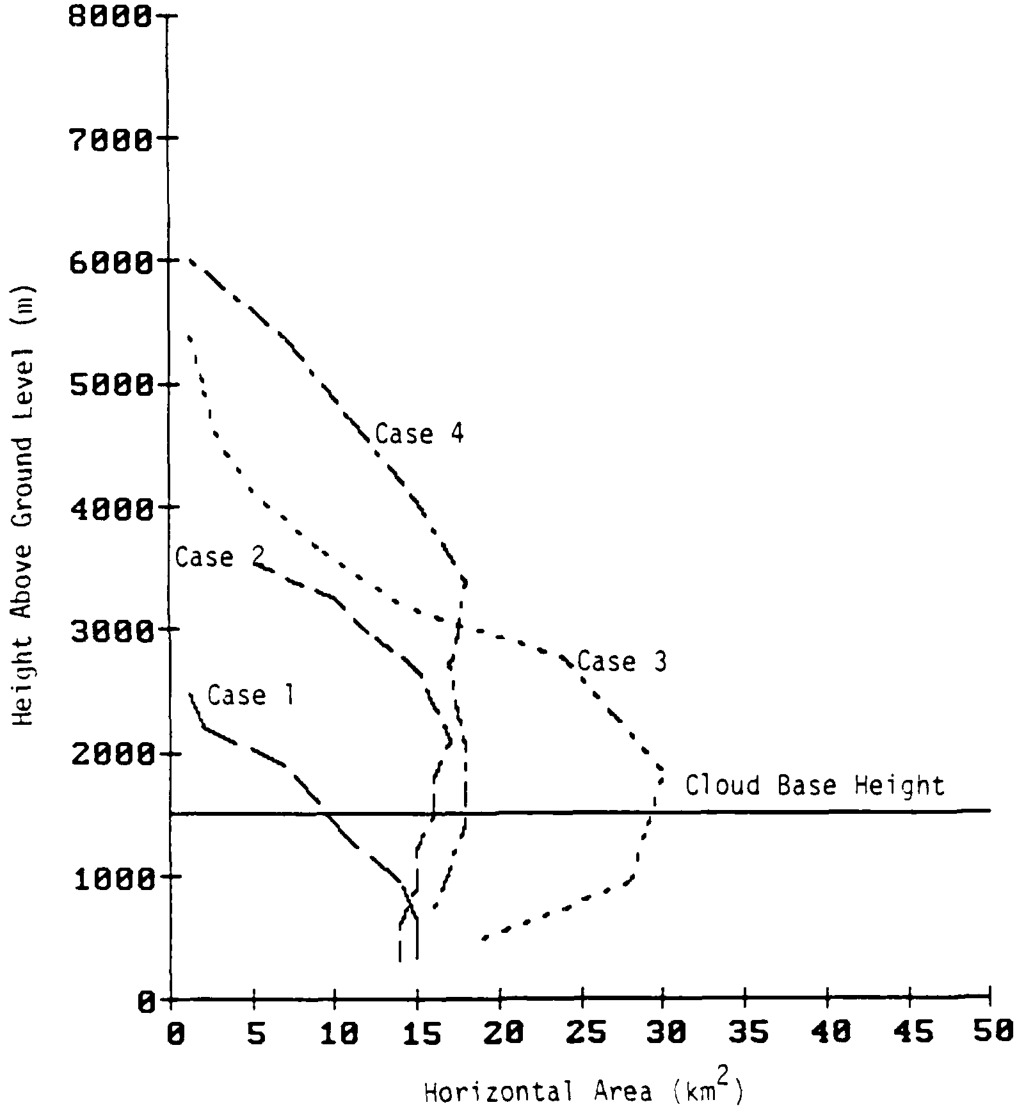

Fig. 7. As in Fig. 5 but recorded one volume scan after the maximum rainfall rate in Fig. 1.

slightly more than that of Case 2, a rainshower, and the smallest in terms of its detected echo height of any of the cases. Since the average reflectivity and horizontal area both increased slightly for Case 2, the possible rationale proposed for Case 3 is inadequate. However, as previously cited, the rainfall-rate estimates derived by radar are strongly dependent upon the time at which the volume scan is taken during the life of a cell. Possibly a volume scan taken 5 minutes either side of Volume Scan 2 (Time Zero in Figure 1) would have recorded a different rainfall rate. As stated previously, because of the 10-minute time span between volume scans, these rainfall rate peaks should not be considered as the absolute maxima that were recorded over the entire life of the cells. They are only rainfall rates relative to given times of volume scans.

6. CONCLUSIONS AND COMMENTS

a. Conclusions

The four cases examined produced profiles of average reflectivity and horizontal area which displayed not only consistent features among the cases relating to average rainfall rate, but characteristics which agreed well with the findings of others. The conclusions reached, which allow several statements to be made concerning the relationship between cell echo signatures and radar-determined average rainfall rates, are based on a small sample size and are, therefore, tentative. These conclusions are presented in two parts.

1) Average reflectivity and radar-derived average rainfall rate

Three conclusions can be drawn concerning the average reflectivity profile of an isolated convective cell and the radar-determined average rainfall rate of the same cell.

a) If the radar reflectivity from the cell, averaged for each level within a volume scan, produces an echo profile which exhibits the highest values at mid levels, then the maximum average rainfall rate determined by radar has not yet occurred.

b) If, on the other hand, an echo profile reveals only decreasing values of average reflectivity from the lowest levels to the top of the echo, then either the maximum average rainfall rate determined by radar is occurring or has occurred.

c) No identifiable characteristic (i.e., change in slope) can distinguish an average reflectivity profile produced during the time of maximum average radar-determined rainfall from one produced after this time except a decrease in magnitude at all levels.

2) Horizontal area and radar-derived average rainfall rate

Two conclusions can be drawn concerning the horizontal area profile of an isolated convective cell and the radar-determined average rainfall

rate of the same cell.

a) If an echo from the cell produces a profile of horizontal area, as defined by the 10-dBz closed contour, that indicates greater horizontal area at mid levels, then the maximum average rainfall rate as determined by radar has not yet occurred.

b) No identifiable characteristic distinguishes the horizontal area profile during the time of maximum average radar-determined rainfall rate from one after this time.

b. Comments

Quite often rainfall-rate estimates determined by radar and those obtained from raingage data do not agree. Since the raingage data are considered as "ground truth" for most comparisons, this discrepancy is usually attributed to inadequacies in the Z-R relationship being applied. The Z-R relationship is an empirical relationship. Therefore, when using it, care must be taken to consider geographic location, type of precipitation, drop-size distribution, height of measurements in the cloud, and other important factors. Well over two dozen different Z-R relationships exist for various applications.

Even when the correct Z-R relationship is applieu in rainfall-rate estimates, another very important consideration can be overlooked. Raingages record only the precipitation that reaches the earth's surface. However, all the precipitation falling from a convective cloud does not necessarily reach the ground. The profiles in Figure 3 indicate that, even during the time of maximum rainfall rate, the average reflectivity differs considerably when values just below cloud base are compared to those at the lowest level. A rainfall-rate estimate from a radar scan taken at an elevation close to the cloud's base could, therefore, be very different from one taken at the lowest possible elevation (i.e., not so low as to cause contamination of the detected signal by the earth's surface).

A radar which has been correctly calibrated can produce rainfall estimates that are very reasonable. But, depending on the specific application and location of the radar, an elevation-scan angle between

0.5 and 0.0 degrees or less might actually produce rainfall-rate estimates of greater accuracy than a scan taken at 1.0 or 1.5 degrees. A scan at 0.0 degrees versus one at 1.0 degrees could mean the difference between sampling the precipitation at the bottom of the rainshaft or sampling it close to the cloud's base.

REFERENCES

Battan, L. J., 1973: Radar Observation of the Atmosphere. The University of Chicago Press, 324 pp.

Dennis, S. A., and A. Kosciepski, 1972: Height and temperature of first echoes in unseeded and seeded convective clouds in South Dakota. J. Appl. Meteor., 11, 994-1000.

Gagin, A., 1980: The relationship between depth of cumuliform clouds and their raindrop characteristics. J. Rech. Atmos., 14, 409-422.

_____, D. Rosenfeld and R. E. Lopez, 1985: The relationship between height and precipitation characteristics of summertime convective cells in south Florida. J. Atmos. Sci., 42, 84-94.

Huebner, G. L., 1987: Personal communication.

Lopez, R. E., 1978: Internal structure and development processes of C-scale aggregates of cumulus clouds. Mon. Wea. Rev., 106, 1488-1494.

_____, D. O. Blanchard, D. Rosenfeld, W. L. Hiscox and M. J. Casey, 1984: Population characteristics, development processes and structure of radar echoes in south Florida. Mon. Wea. Rev., 112, 56-75

Malkus, J. S., and R. H. Simpson, 1964: Modification experiments on tropical cumulus clouds. Science, 145, 541-548.

Riggio, R. F., W. O. Alexander, T. J. Larkin and G. W. Bomar, 1983: Texas HIPLEX Summary Report, 1975-1980. Texas Department of Water Resources, 176 pp.

Simpson, J., and W. L. Woodly, 1971: Seeding cumulus in Florida: New 1970 results. Science, 172, 117-126.

Warner, J., 1977: Time variation of updraft and water content in small cumulus clouds. J. Atmos. Sci., 34, 1306-1312.

VITA

Terry Alvin Huber was born in Stamford, Texas, on 5 October 1950. He was the first born of "Buck" and Mary Huber.

After entering the United States Navy in 1970, he was trained as a diesel mechanic and served in the "black gang" aboard two Navy ships: the U.S.S. Schnectady and the U.S.S. Cleveland. He served two tours in Vietnam and was awarded the Navy's Combat Action Ribbon in 1973.

After leaving the Navy in May 1974, he entered college. In December 1978, he received a Bachelor of Science degree in Physics from Angelo State University, San Angelo, Texas,

He attended the Officer Training School (O.T.S.) at Lackland Air Force Base (AFB), San Antonio, Texas, and was commissioned a Second Lieutenant in the United States Air Force on 25 May 1979. In the fall of 1979, he reported for training in the Basic Meteorology program at Texas A&M University, College Station, Texas. His first weather assignment was to Detachment 7, 17th Weather Squadron at Kelly AFB, San Antonio, Texas. He was promoted to First Lieutenant in May 1981. In September 1982 he returned to O.T.S. as an instructor and was promoted to Captain in May 1983.

He returned to Texas A&M in the Fall of 1985 to begin work on a Master of Science Degree in Meteorology under an Air Force scholarship.

Captain Huber's permanent mailing address is: 66 E. 18th St., San Angelo, Texas.

END
DATE
FILMED
DEC.
1987